

LATTICE DESIGN OF A PULSED SYNCHROTRON CHAIN FOR A MUON COLLIDER SITED AT FERMILAB*

K. G. Capobianco-Hogan[†], Stony Brook University, Stony Brook, NY, USA
 J. S. Berg, Brookhaven National Laboratory, Upton, NY, USA

Abstract

We present preliminary lattices for a rapid cycling synchrotron (RCS) chain based on a bottom up design for a 10 TeV parton center-of-momentum (pCM) muon collider sited at Fermilab. The smallest RCS rings in this lattice are 6.28 km in circumference and the largest RCS ring fitting fully within the Fermilab site is 15.5 km. To reach 5 TeV per beam, a single tunnel containing up to two rings is allowed to exceed the 15.5 km limit. Each ring is either a conventional RCS or a hybrid RCS. A conventional RCS relies on only iron dominated, ramped field magnets while a hybrid RCS relies on a combination of interleaved ramped field and superconducting fixed field magnets to achieve higher average magnetic fields while maintaining the high ramp rates achievable with iron dominated magnets. A pair of 6.28 km RCS rings and a 15.5 km RCS ring accelerate beams from 63 GeV to 1.54 TeV. Three scenarios for acceleration from 1.54 TeV to 5 TeV using an off-site tunnel are presented.

INTRODUCTION

Our goal is to design a rapid cycling synchrotron (RCS) acceleration chain from 63 GeV to 5 TeV for muon and anti-muon beams as part of a Fermilab sited muon collider. Here, we present three preliminary designs to accomplish this using four to five RCS rings. All three scenarios rely on the same designs for the first three rings (which would fit within the Fermilab site) to reach an energy of 1.54 TeV. The scenarios differ in how they accelerate beams from 1.54 TeV to 5 TeV.

The existing Tevatron tunnel located on the Fermilab site has a circumference of 6.28 km. We use this as the circumference of the first two rings (RCS 1 and RCS 2), though further analysis is required to determine if the rings would in fact fit within the Tevatron tunnel. We estimate the maximum circumference that can fit on the Fermilab site to be 15.5 km, which we use for the third ring (RCS 3).¹ A single tunnel (containing one or two rings, depending on scenario) is allowed to go beyond the Fermilab site boundary to reach an energy of 5 TeV per beam, with the circumference of the final tunnel being optimized to do so.

Each ring is divided into either six or twelve superperiods. As shown in Fig. 1, each superperiod consists of a straight section, an arc section, and two dispersion suppressor sections (which connect the straight and arc sections).

Straight section consists of n_{RF} straight cells containing RF cavities, with an additional two utility straight cells in six of the straight sections. Arc sections consist of n_{arc} arc cells. A half-bend dispersion suppressor scheme is used, with each dispersion suppressor section consisting of two dispersion suppressor cells — nominally, arc cells with bending fields reduced by approximately 50 %. We optimize the number of superperiods per ring, the number of arc cells per superperiod, and the number of RF straights per superperiod to maximize the extraction energy of each RCS while keeping other lattice parameters within reasonable limits.

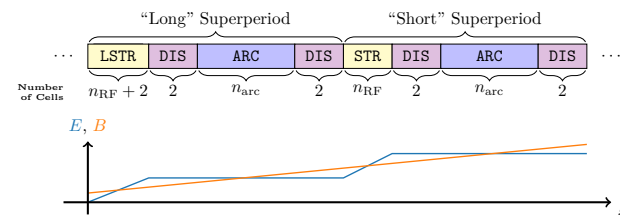


Figure 1: Above, a superperiod consists of either a “long” (LSTR) or “short” (STR) straight section, an arc section (ARC), and a pair of dispersion suppressor sections (DIS). Below, a sketch of intermittently ramped beam energy (blue) and continuously ramped magnetic field (orange) as a function of beam position depicts the mismatch between beam energy and ramped magnet field.

CONSTRAINTS AND ASSUMPTIONS

For our designs, we assume that ramped dipole bend magnets can reach fields of 1.75 T [1] and (following a “2/3 rule”) that ramped quadrupole magnets can reach pole tip fields of 1.2 T. While these fields are sufficient for the lowest energy ring (RCS 1), they would result in excessively large rings at higher energies.² To limit the footprint of the RCS chain, fixed field superconducting magnets are interleaved with ramped magnets, achieving higher average fields, as shown in Fig. 2. Pole-tip field levels should be under 14 T for fixed field superconducting bend magnets and maximum pole tip fields of 12.5 T for fixed field superconducting quadrupoles [2].

A betatron phase advance per cell of 90° was chosen to facilitate the inclusion of sextupole magnets if chromatic corrections are necessary. Dispersion suppressor cells and the arc and straight cells adjacent to them are exempt from the 90° phase advance requirement as their quadrupole magnets are used for matching between the arc and straight sections.

* This manuscript has been authored by employees of Brookhaven Science Associates, LLC under Contract No. DE-SC0012704 with the U.S. Department of Energy.

[†] kyle.capobianco-hogan@stonybrook.edu

¹ In Scenario B, the fourth ring (RCS 4B, see Scenarios) shares the 15.5 km tunnel with RCS 3.

² Nearly 60 km of bending dipoles would be required for a ring to reach an energy of 5 TeV per beam.

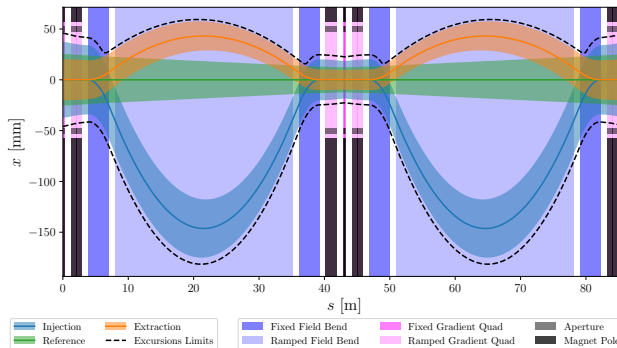


Figure 2: An RCS 3 arc cell with 5σ beam size and dashed curves indicate the estimated variation in orbits due to the mismatch between beam energy and ramped magnet fields. Interleaved fixed field and ramped field bends are indicated in blue and light blue, respectively.

Quadrupole apertures are sized to accommodate 5σ beams with normalized transverse emittance of 0.025 mm. Because beam energy is ramped intermittently (only when passing through RF straights) while magnet fields are ramped continuously, there is a mismatch between beam energy and magnet field. The excursions resulting from this energy-field mismatch are estimated as $\eta_x \Delta E_{\text{sup}} / 2E$, which is included in the calculation of aperture requirements. The pole tip of quadrupole magnets is assumed to be 10 mm beyond their apertures.

For our RF calculations, we assume cavities operate at 1.3 GHz and 25 MV/m. For each RCS, we initially use an estimated relative momentum spread σ_{p_z} to calculate required quadrupole apertures and optimize quadrupole lengths. We then calculate the momentum compaction factor, which we use to calculate the synchronous phase required to match a 5σ beam with a longitudinal emittance of 0.025 eV s into an RF bucket. This gives us enough information to calculate the relative momentum spread. We then use this calculated relative momentum spread to re-optimize the lattice, repeating the process until the relative momentum spread converges.

The analytic model we used to calculate the RF parameters relies on an approximation that acceleration is continuous, which is valid in the limit where the synchrotron tune per superperiod is much less than $1/\pi$. For purposes of our analysis, we exclude ring parameters that result in a synchrotron tune per superperiod greater than 0.15.

To limit decays, we use an average accelerating gradient of 2.5 MV/m in RCS 1. In RCS 2 and 3, the average accelerating gradient is reduced to 2.0 MV/m to improve dipole packing fraction. In the rings used to accelerate from 1.54 TeV to 5 TeV, the average accelerating gradient is further reduced to 1.0 MV/m.

Based on [3], we assume kicker dipoles can reach a field of 0.2 T in order to estimate the required kicker lengths needed for injection and extraction using the single turn scheme. We approximate the values of β_x at the kicker and septum with the average of the minimum and maximum values of β_x in a straight cell. Based on the forgoing, a pair of utility

straight cells can comfortably accommodate an injection or extraction unit.

OPTIMIZATION

While the required quadrupole length to achieve a betatron phase advance of 90° per cell increases with cell length, the fraction of a cell occupied by quadrupoles decreases with cell length. Therefore, maximizing cell length minimizes the quadrupole packing within cells while maximizing dipole packing in arc and dispersion suppressor cells as well as RF cavity packing within straight cells.

We take all cells to be the same length in our current design. The larger the arc cells become (in order to maximize dipole packing within the cell), the larger the straight cells and dispersion suppressor cells become. Longer straight cells are able to accommodate more RF cavities, and consequently, reduce the number of straight cells needed for RF cavities. However, longer straight cells cause the twelve utility straight cells to occupy a larger fraction of the ring.

Similar to utility straights, the number of dispersion suppressor cells is independent of the cell length (at four cells per straight section). However, unlike utility straights, dispersion suppressor cells do contribute to bending, but only making half the contribution of arc cells. As a consequence, while the fraction of arc cells occupied by bending magnets increases monotonically with cell length, the dipole packing fraction of the ring reaches a maximum. Despite this, RCS 2 uses only four arc cells per superperiod, which is the minimum we allow in this analysis.

The number of superperiods is likewise optimized to maximize the dipole packing fraction. The greater the number of superperiods, the smaller the synchrotron tune per superperiod becomes, up to variations dependent on the number of arc cells per superperiod. Therefore, the number of superperiods has an “approximate” lower bound³ since the synchrotron tune per superperiod must be less than or equal to 0.15. Similarly, the mismatch between beam energy and ramped magnet field (Fig. 1) decreases with the number of superperiods, but unlike the former, the mismatch is not restricted by a hard limit, but is instead limited indirectly as a result of its contribution to quadrupole aperture requirements. Because an increased number of superperiods decreases the energy-field mismatch’s contribution to quadrupole aperture but also increases the number of dispersion suppressor cells, there is an optimal number of superperiods that maximizes the extraction energy of the ring. Table 1 summarizes this effort.

SCENARIOS

We present three scenarios to accelerate beams from 1.54 TeV to 5 TeV, each with their own advantages and disadvantages. All three scenarios use the same design for the

³ The lower bound is “approximate” in that it is dependent on the number of arc cells per superperiod.

Table 1: Parameters of RCS Chains

Parameter	RCS 1	RCS 2	RCS 3	RCS 4A	RCS 4B	RCS 5B	RCS 4C	RCS 5C
Hybrid RCS	No	Yes	Yes	Yes	Yes	Yes	Yes	Yes
Injection energy (TeV)	0.063	0.174	0.454	1.54	1.54	2.71	1.54	3.46
Extraction energy (TeV)	0.174	0.454	1.54	5.00	2.71	5.00	3.46	5.00
Energy ratio	2.76	2.61	3.39	3.24	1.76	1.85	2.25	1.44
Circumference (km)	6.28	6.28	15.5	35.4	15.5	26.8	21.9	21.9
Number of superperiods	12	12	12	6	6	6	6	6
RF cells per superperiod	4	2	2	3	2	2	2	2
arc cells per superperiod	8	4	8	38	24	30	28	28
Packing fraction, ramped bend (%)	33.1	26.7	42.0	58.4	45.1	51.1	52.5	41.9
fixed bend (%)	0	7.48	9.63	13.8	20.5	21.5	17.1	28.9
quad (%)	57.9	11.0	8.05	5.30	4.07	3.40	4.37	3.02
Average accelerating gradient (MV/m)	2.50	2.00	2.00	1.00	1.00	1.00	1.00	1.00
Synchronous phase ⁴ (°)	57.0	57.2	43.0	32.4	37.9	31.9	36.1	31.1
Superperiod synchrotron tune (10^{-2})	6.91	5.85	4.47	3.87	3.28	3.15	3.72	2.53
$\sigma_{p_z} (10^{-4})$	136	49.2	25.5	10.1	8.5	5.80	8.98	4.65
$\Delta E_{\text{sup}}/E_{\text{inj}} (10^{-4})$	208	60.3	56.9	38.3	16.8	16.5	23.7	10.5
Survival rate	0.937	0.926	0.907	0.828	0.913	0.906	0.878	0.943
Total survival rate	0.937	0.867	0.786	0.651	0.718	0.651	0.691	0.651
Number of turns	7.04	22.3	35.1	97.6	75.4	85.3	87.7	70.0
Acceleration time (ms)	0.148	0.468	1.81	11.5	3.90	7.64	6.42	5.12
Injection kicker length (m)	0.861	1.31	1.73	3.33	4.74	5.55	3.93	7.77
Extraction kicker length (m)	1.81	2.70	4.50	8.89	7.66	9.40	7.77	10.71
Utility drift length ⁵ (m)	12.0	19.4	38.6	58.1	35.4	53.8	45.9	45.3

first three rings (RCS 1–3) — which accelerate beams to an energy of 1.54 TeV on the Fermilab site.

Scenario A uses a single ring (RCS 4A) measuring 35.4 km to accelerate beams from 1.54 TeV to 5 TeV. This scenario minimizes the total length of the acceleration chain, but requires a ring more than twice as large as can be fit within the Fermilab site.

Scenario B uses an additional on-site ring (RCS 4B) measuring 15.5 km to reach 2.71 TeV followed by an off-site ring (RCS 5B) measuring 26.8 km to reach 5 TeV. It increases the maximum energy that can be reached on the Fermilab site while decreasing the circumference of the off-site tunnel compared to Scenario A, but also increases the overall length of the RCS chain.

Scenario C uses a pair of off-site rings (RCS 4C and RCS 5C) in a shared tunnel measuring 21.9 km in circumference to reach 5 TeV. It further reduces the circumference of the off-site tunnel, but slightly increases the overall length of the chain compared to Scenario B.

CONCLUSION

These designs demonstrate that it is likely feasible to reach an energy of more than 2.5 TeV per beam (5 TeV pCM) within the limits of the Fermilab site and to reach the target energy of 5 TeV per beam (10 TeV pCM) with the addition of a single tunnel going beyond the Fermilab site boundary.

Future Work

In hybrid RCS rings, beams are (depending on their energy) over- or under-bent by fixed field dipoles during the course of a ramp. These steering errors are corrected for by ramped field dipoles, but still result in energy dependent orbital excursions. The current designs use a single hybrid bend unit⁶ per half-cell in hybrid RCS rings. Given the large cell lengths employed by these designs, the hybrid bend units and the orbital excursions may be large enough to warrant mitigation. In past iterations of the RCS design, we have evaluated the use of multiple hybrid bend units per half-cell as a means of doing so [4]. While this method does reduce excursion magnitude, it also reduces dipole packing and energy range, which will necessitate an increase in circumference of the final tunnel, a decrease in final beam energy, variation of other parameters to compensate, or a combination of the above.

More detailed analysis of the design and tracking simulations are necessary to evaluate the effects of the mismatch between beam energy and ramped magnet fields and verify that quadrupole apertures are sufficient to accommodate the excursions. Tracking simulations must also be performed to determine if chromatic correction is necessary. RF matching between the rings and its effect on longitudinal emittance must also be simulated and studied. These designs will continue to update and evolve based on the results such analysis.

⁴ A “hybrid bend unit” consists of a single ramped bend dipole between a pair of fixed field bend dipoles.

⁵ Two utility drifts per straight cell.

REFERENCES

- [1] J. S. Berg and H. Witte, “Pulsed synchrotrons for very rapid acceleration”, *AIP Conference Proceedings*, vol. 1777, no. 1, p. 100 002, 2016. doi:10.1063/1.4965683
- [2] L. Bottura, F. Boattini, B. Caiffi, S. Mariotto, L. Quettier, and M. Statera, “Muon collider WP7 - magnets”, presented at Accelerator design meeting, Dec. 2022. https://indico.cern.ch/event/1219424/contributions/5129969/attachments/2564512/4424496/MC_magnets_status_v1.pdf
- [3] E. Nakamura, “Fast-rise high-field kicker magnet operating in saturation”, *Nuclear Instruments and Methods in Physics Research Section A: Accelerators, Spectrometers, Detectors and Associated Equipment*, vol. 612, no. 1, pp. 50–55, 2009. doi:10.1016/j.nima.2009.08.090
- [4] K. G. Capobianco-Hogan and J. S. Berg, “Lattice design of a pulsed synchrotron for a muon collider fitting within the fermilab site boundary”, in *Proc. IPAC’24*, Nashville, TN, pp. 448–451, 2024.
doi:10.18429/JACoW-IPAC2024-MOPR01